

NATIONAL ADVISORY COMMITTEE FOR AERONAUTICS.

TECHNICAL MEMORANDUM NO. 422.

SYSTEMATIC INVESTIGATION OF JOUKOWSKY WING SECTIONS.*

By O. Schrenk.

During the last few years the Göttingen Aerodynamic Institute was prevented by purely economic reasons from undertaking extensive investigations. Ackeret, however, began systematic polar measurements on Joukowski wing sections, which were occasionally conducted in the wind tunnel when this could be conveniently done without interfering with current work. Under these conditions a considerable number of wing sections were tested during the last four years and the tests are now more or less concluded.

Ackeret explained the purpose of his investigations in a lecture delivered before the W. G. L. (Wissenschaftliche Gesellschaft für Luftfahrt) in 1924. He also announced some of the preliminary results (see N.A.C.A. Technical Memorandum No. 323). These tests were expected to yield certain general information regarding the aerodynamic behavior of wings of different thickness and camber, especially for extreme shapes, and also to determine the systematic differences between the wing-section theory which neglects the friction (Joukowski theory) and the actual behavior of the Joukowski sections (J-sections). These

*Systematische Untersuchungen an Joukowski-Profilen. From "Zeitschrift für Flugtechnik und Motorluftschiffahrt," May 28, 1927, pp. 225-230.

two questions form the subject of the present report.

The bare results have just been published in Report III of the Göttingen Aerodynamic Institute. The theoretical results and their detailed presentation will be contained in a report to appear shortly in "Zeitschrift für Flugtechnik und Motorluftschiffahrt." We shall refer but briefly to the theory and only when absolutely necessary.

Fig. 1 shows the tested sections. It will be remembered that all the J-sections were obtained by the same method. They all have the same general shape and differ only in thickness and camber. Their distinctive features include the rounded leading edge, the upward camber of the lower surface toward the rear and the very thin trailing edge. Two characteristic parameters belong to each J-section: one for the camber, usually denoted by f/l , and one for the thickness, for which we shall adopt the symbol d/l , as better suited for our purpose than the parameter δ/l introduced by Trefftz (Z.F.M. 1913, p. 130); $\frac{d}{l} = \frac{2\delta}{l}$.

The exact signification of the parameters results from the theory of the J-sections. The parameters can also be determined with fair accuracy from the dimensions of a given Joukowski section or any other section of similar shape. For this purpose a central curve is drawn between the suction side/and the pressure side (lower camber) from the leading edge to the trailing edge and equated by an arc. Except for small deviations,

f/l is then the ratio of the departure of the curve from the chord to half the length of the chord of the arc (Fig. 2).

d/l is then approximately the ratio of the maximum thickness to the chord of the section. A more accurate idea of this relation is obtained from the following table:

$\frac{d}{l}$	0.05	0.10	0.15	0.20	0.25
Thickness/chord	0.06	0.12	0.17	0.21	0.26

The experiments were carried out with standard wings (20 x 100 cm) at wind velocities of 15 and 30 m/sec. It should be stated beforehand that a systematic influence of the wind velocity could be traced only in one respect, namely, in wing section drag. It is a well-known fact that this drag is often 10 to 40% higher at 15 m/sec than at 30 m/sec. Therefore, in the rest of this article, we shall only refer to measurements at 30 m/sec.

We shall first consider the wing-section drag. Calculations according to Joukowsky lead to a zero wing-section drag, since the friction and hence the tangential wing forces and the formation of vortices behind the wing are not taken into consideration. In Figs. 3 to 7 the magnitude of the wing-section drag $c_{w\infty}$ is plotted in the usual way against the lift for a certain number of wing-section groups of equal thickness but different camber. For greater clearness each of the three values of the thickness $\frac{d}{l} = 0.10 = 0.15$, and 0.20 was di-

vided into two groups. An elliptical lift distribution was assumed for all the calculations, and no particular accuracy can therefore be claimed for highly cambered sections owing to their irregular behavior. Besides, in this case there is an absolute lack of reliable data for a more accurate calculation. In Fig. 8 the minimum drag for each section is plotted against d/l and f/l , the highly cambered sections having been omitted. The two diagrams in Fig. 8 give, as a whole, a good idea of the behavior of the wing-section drag and of its sensitivity to changes of thickness and camber. It would, however, be useless to attempt to explain all the bumps and intersections of the curves. Secondary influences must also be taken into consideration, such as the flow in the boundary layer, which it has hitherto been impossible to calculate, or perhaps slight changes in the suspension and wing structure. In Fig. 8 all these disturbances appear to have such high values, because the scale used for $c_{w\infty}$ is much larger than usual.

The behavior of the lift is also important. For the flow of a frictionless fluid in the case of a wing with infinite span, the lift coefficient can be calculated by

$$c_a = 2 \pi \frac{D}{t} \sin \alpha_{th\infty}$$

or, since in this case the angles of attack are comparatively small, approximately by

$$c_a = 0.11 \frac{D}{t} \alpha_{th\infty}$$

The numerical values of D/t which differ for each section are given in Report III of the Göttingen Aerodynamic Institute. They vary between 1.05 and 1.20. The diameter D of a circle is a very important factor of the theory, and t is the chord. α_{th} is the "theoretical angle of attack," that is, the angle measured from the theoretical line of zero lift. α_{th} is usually a few degrees greater than the normal angle of attack α . $\delta = \alpha_{th} - \alpha$, the difference between the angles, is also given in Report III. The symbol ∞ was added to denote the angle of attack of a wing with infinite span.

For the comparison of measurement and theory, the theoretical angle of attack was first converted to the experimentally tested aspect ratio of 5 : 1, that is, the angle of attack was simply corrected according to the wing theory. In order to simplify the method of representation, all c_a values, both experimental and calculated, were divided by the corresponding D/t . Owing to this reduction and to the conversion according to the aspect ratio, the following value was obtained for the theory:

$$\frac{c_a}{D/t} = c_{a\text{red.}} = 0.079\alpha_{th}$$

The test values can no longer be compared among themselves after reduction, each section having been converted with a special value of D/t , but they can all be compared to the one theoretical curve $c_a = 0.079\alpha_{th}$ (Figs. 9-11). This representation

shows that there is a certain number of wing-section shapes, chiefly those with a small camber and a value of $f/l \leq 0.1$, whose lift c_a , aside from slight deviations of the zero point, is approximately proportional to the theoretical angle of attack and hence to the theoretical lift. These low-camber sections have in general a more regular behavior than the others. Their $c_a - c_{w\infty}$ curves run with a rather constant $c_{w\infty}$ value through the axis $c_a = 0$, without deviating to the right before reaching this axis, and their moment lines run straight to this axis (Report III). It can be assumed that these three phenomena are all due to the same cause. The quality of the flow of these low-camber sections is probably the same (i. e., constant) in the domain of positive lift and up to the upper point where the flow separates, whereas for the other sections the flow separates on the lower surface for small lift values.

Hence the following relation can be established for low-camber sections:

$$c_a = \frac{D}{t} k_{\infty} \alpha_{th\infty}$$

and correspondingly, for an aspect ratio of 5 : 1,

$$c_a = \frac{D}{t} k \alpha_{th}$$

The experimental values of k_{∞} and k are always smaller than the theoretical ones. The difference amounts to about 15% for

the better wing sections (see the following table). The values which most closely approximate the theory are those obtained with wing sections of medium thickness.

d/l	f/l			Wing-section number	k_{∞}	k	k or k_{∞} in % of theoret. value
0.05	0	-	-	537 - -	0.088	0.063	80
0.05	0.10;	-	-	558 - -	0.096	0.069	87
0.10	0;	0.05;	0.10	429; 541; 580	0.096	0.069	87
0.15	0;	0.05;	0.10	538; 555; 433	0.092	0.066	83
0.20	0;	0.05;	0.10	539; 556; 434	0.087	0.063	80
0.25	0;	0.10;	-	540; 435; -	0.084	0.060	75

From this table the first approximation formula for the determination of the experimental lift for any wing section of usual shape for the aspect ratio 5 : 1 is derived as follows:

$$c_a = 0.07 \alpha_{th}$$

and for the aspect ratio ∞ : 1

$$c_a = 0.1 \alpha_{th\infty}$$

It appears that these formulas are also approximately correct for other usual section types.

Fig. 12 shows the maximum lift coefficients of the polars. The high degree of dispersion is due to the well-known fact that the separation process is subject to strong disturbing influences and can not therefore be accurately determined. It can be seen, however, that the maximum lift greatly increases with the camber, and that the influence of the wing-section thickness is very small. This influence is only apparent on

very thin sections ($\frac{d}{l} = 0.05$), which have a slightly smaller maximum lift.

Lastly, a very simple determination can be made regarding the moment of the lifting power on the wing. In order to obtain a comparison of theory and measurement, the theoretical moment line was plotted together with the experimental line in the diagrams in Report III. It was found, however, that a better representation of the conditions is obtained by determining the theoretical and experimental working points of the force for a given angle of attack, instead of comparing the c_m values for the same lift. As a matter of fact, it appeared that, within the convenient region of the section, i.e., where the wing-section drag is small, the theoretical center of pressure coincides very closely with the experimental center of pressure, especially for mean values of the lift. Naturally, the angle of attack for the theoretical calculation must be first reduced to the aspect ratio 5 : 1 and, inversely, the experimental angle of attack to the two-dimensional case.

This determination of the constancy of the center of pressure may occasionally form the basis of various considerations. It may, for instance, be applied to the preliminary determination of the actual velocity and pressure distribution on wings of finite span and arbitrarily chosen wing sections by using

the theoretical calculation methods indicated by Trefftz.*
Hitherto, these methods could only be applied to the calculation of a two-dimensional, frictionless flow.

Translation by
W. L. Kaporinde, Paris Office,
National Advisory Committee
for Aeronautics.

* "Zeitschrift für Flugtechnik und Motorluftschiffahrt," 1913,
p. 130.

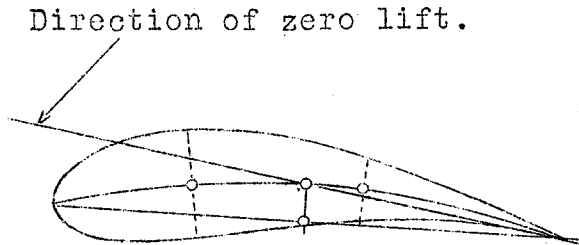


Fig.2 Determination of camber coefficient f/z of a wing section.

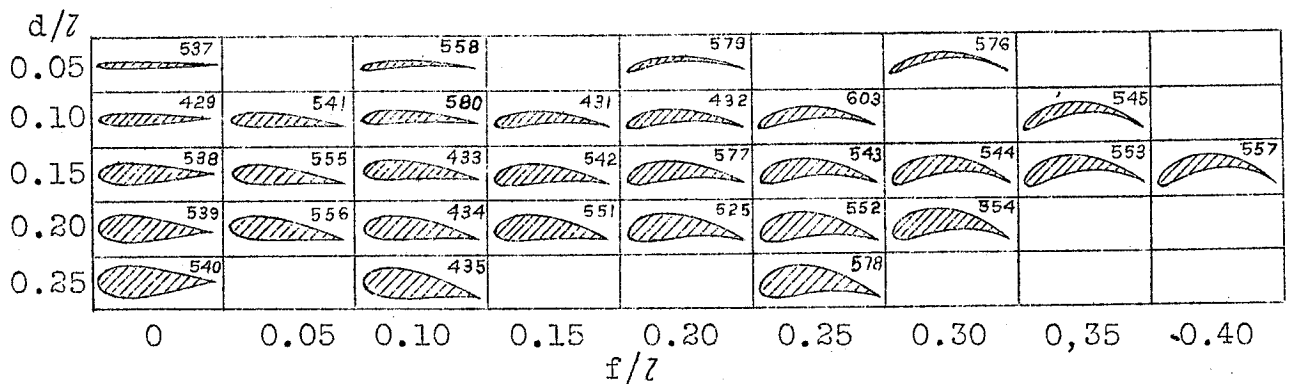


Fig.1 Tested Joukowski sections arranged according to camber and thickness.

● Profile 540, $f/z = 0.00$
 ○ " " 435 " = 0.10
 × " " 578 " = 0.25

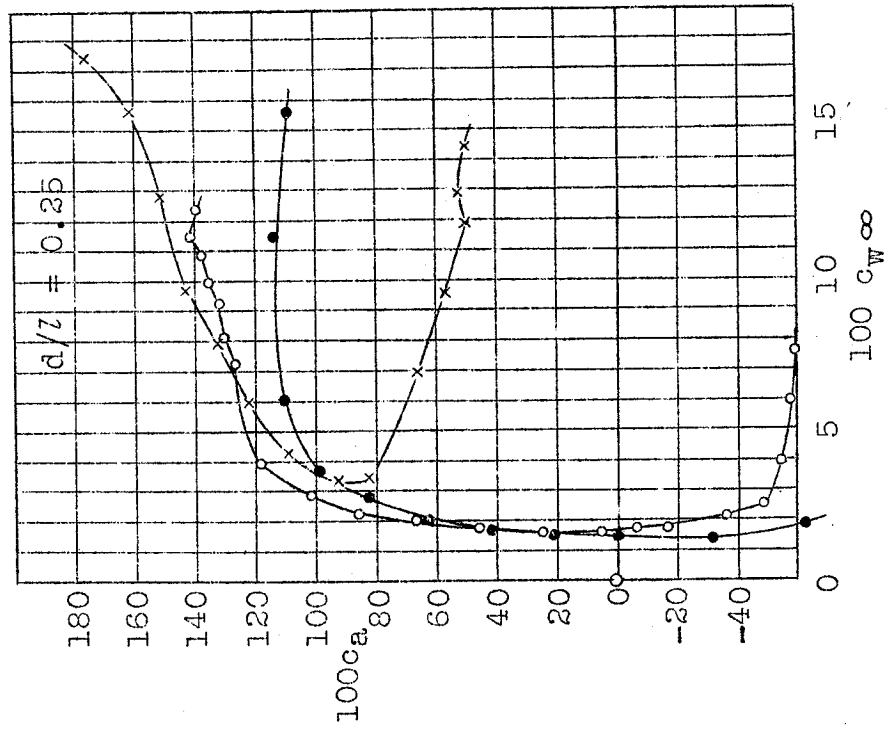


Fig.7 Wing-section drag $c_{w\infty}$ plotted against lift c_a .

× Profile 537, $f/z = 0.00$
 ○ " " 558, " = 0.10
 ● " " 579, " = 0.20
 + " " 576, " = 0.30

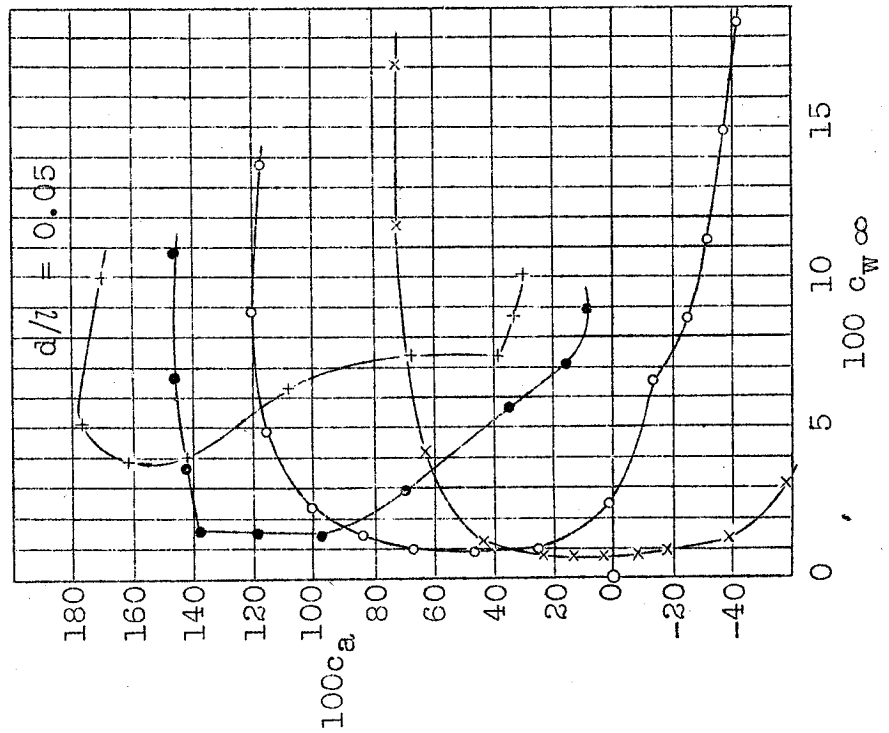


Fig.3 Wing-section drag $c_{w\infty}$ plotted against lift c_a .

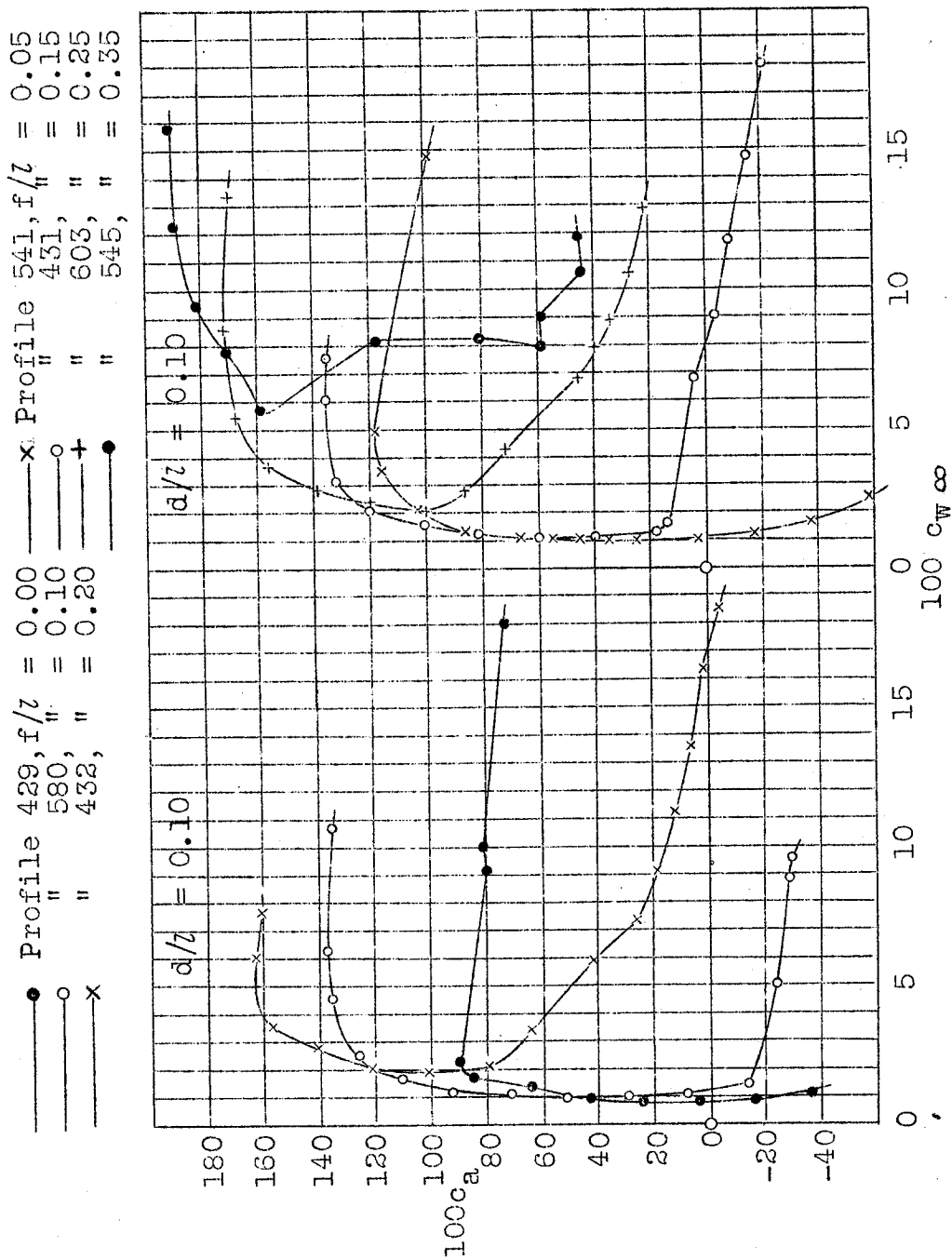


Fig.4 Wing-section drag $c_{w\infty}$ plotted against lift c_a .

—x—	Profile 538,	$f/z = 0.00$	○	Profile 555,	$f/z = 0.05$
—○—	" 433,	" = 0.10	+	" 542,	" = 0.15
—●—	" 577,	" = 0.20	x	" 543,	" = 0.25
—+—	" 544,	" = 0.30	●	" 553,	" = 0.35
—○—	" 557,	" = 0.40			

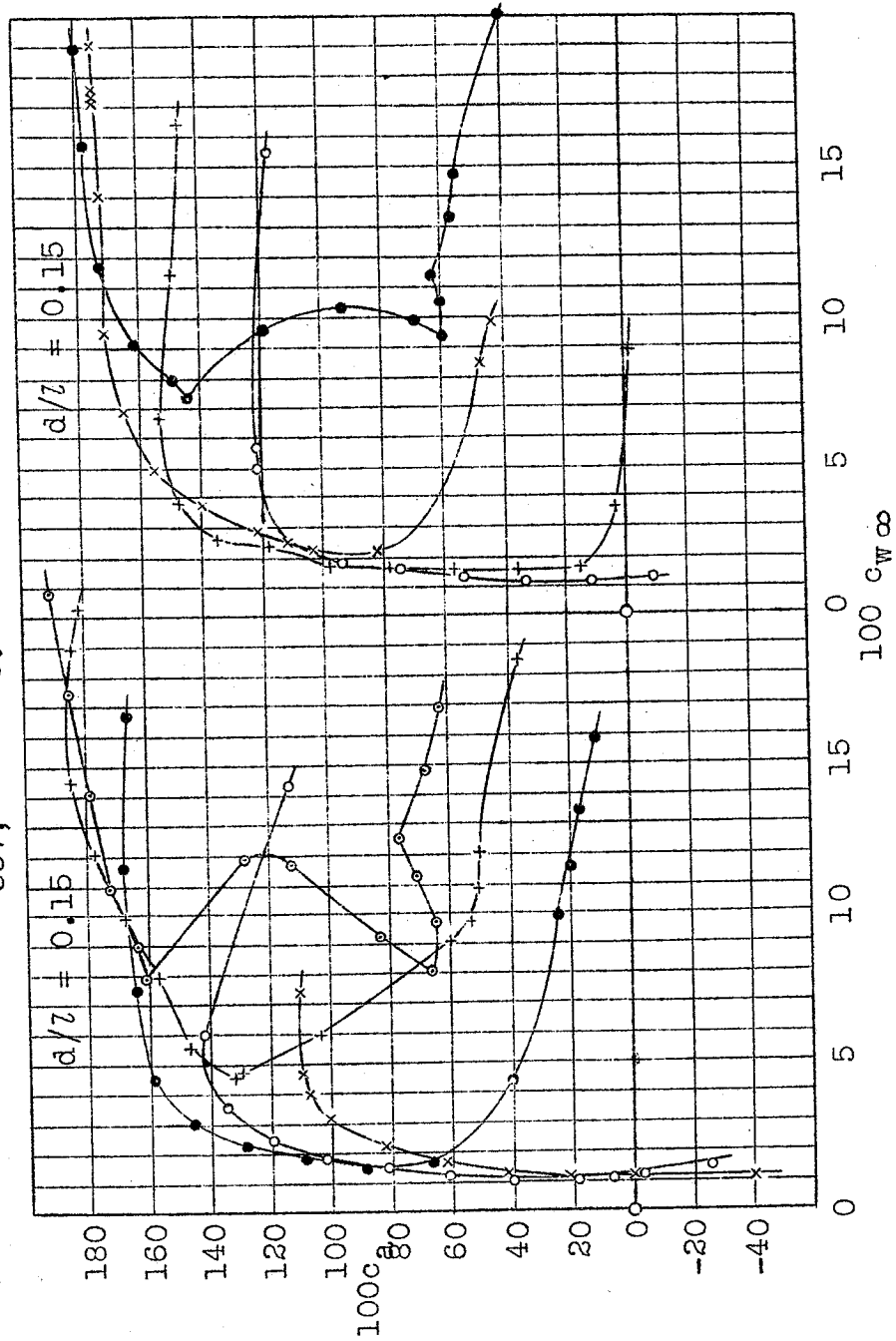


Fig.5 Wing-section drag c_w plotted against lift c_l .

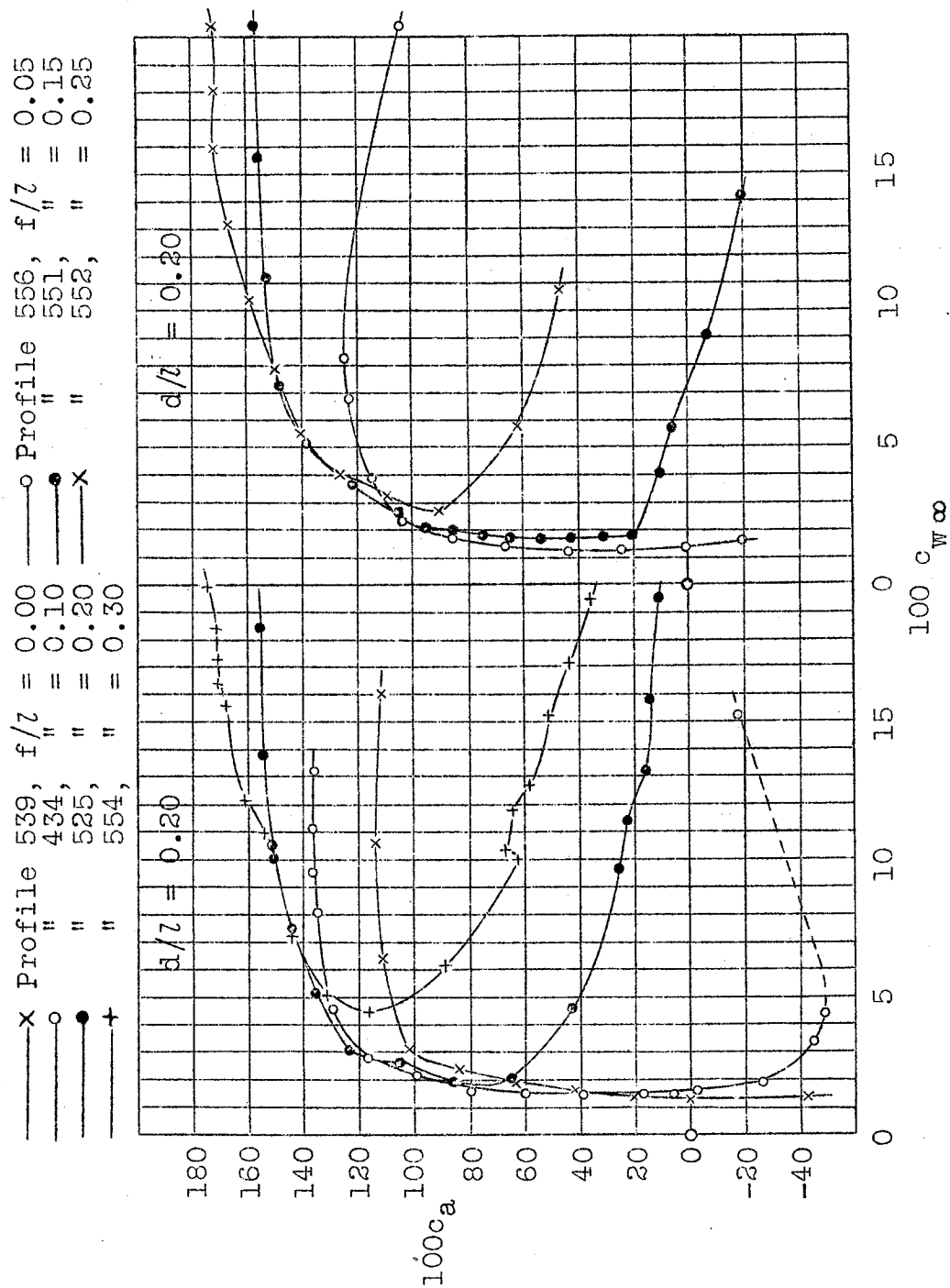


Fig.6 Wing-section drag $c_{w\infty}$ plotted against lift c_a .

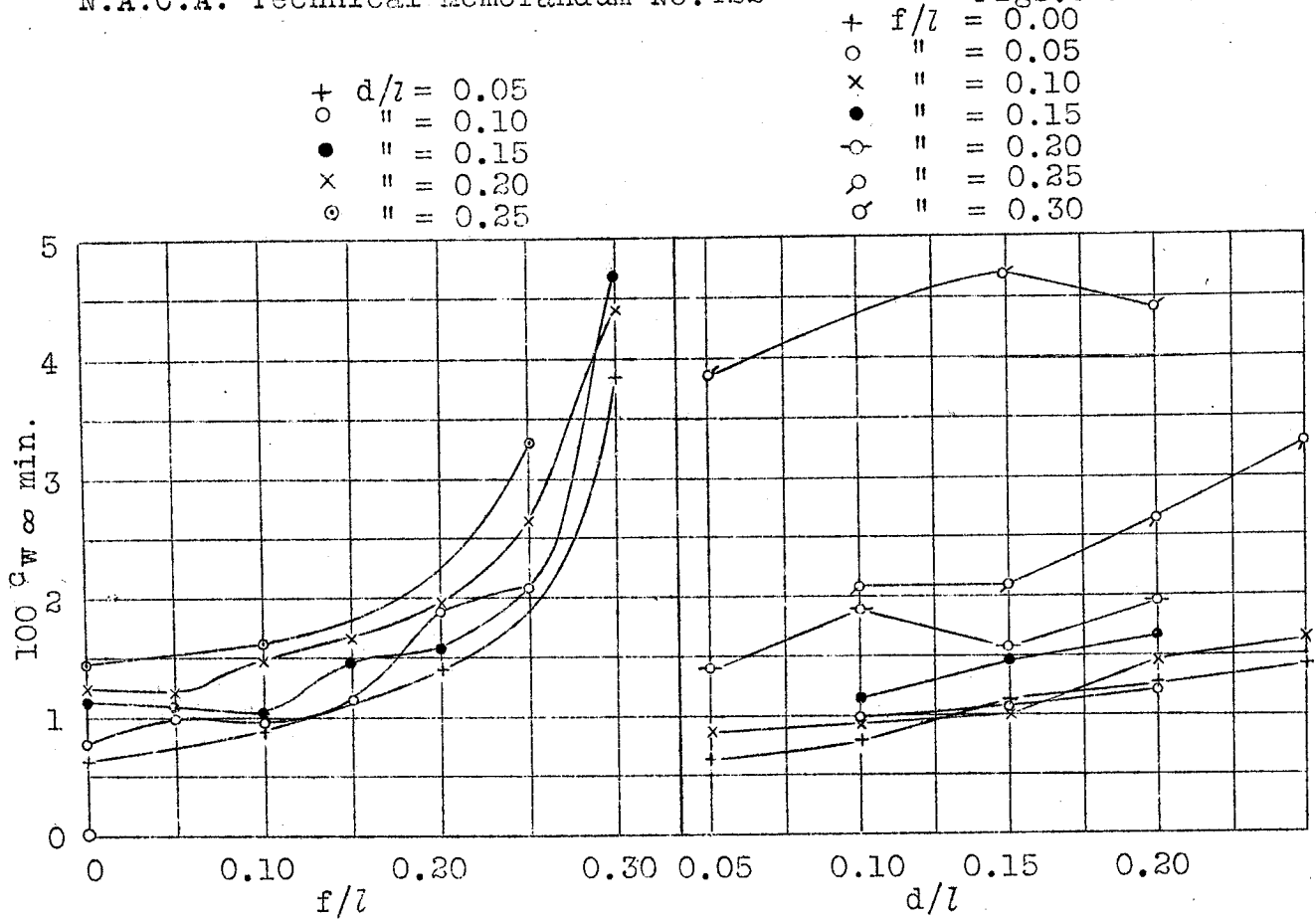
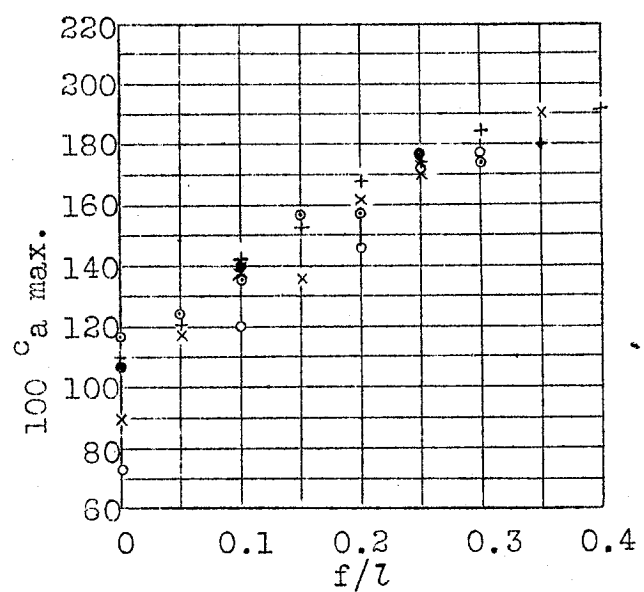


Fig.8 Minimum section drag plotted against f/l and d/l .

Fig.12 $c_{a \text{ max}}$ plotted against wing-section camber.



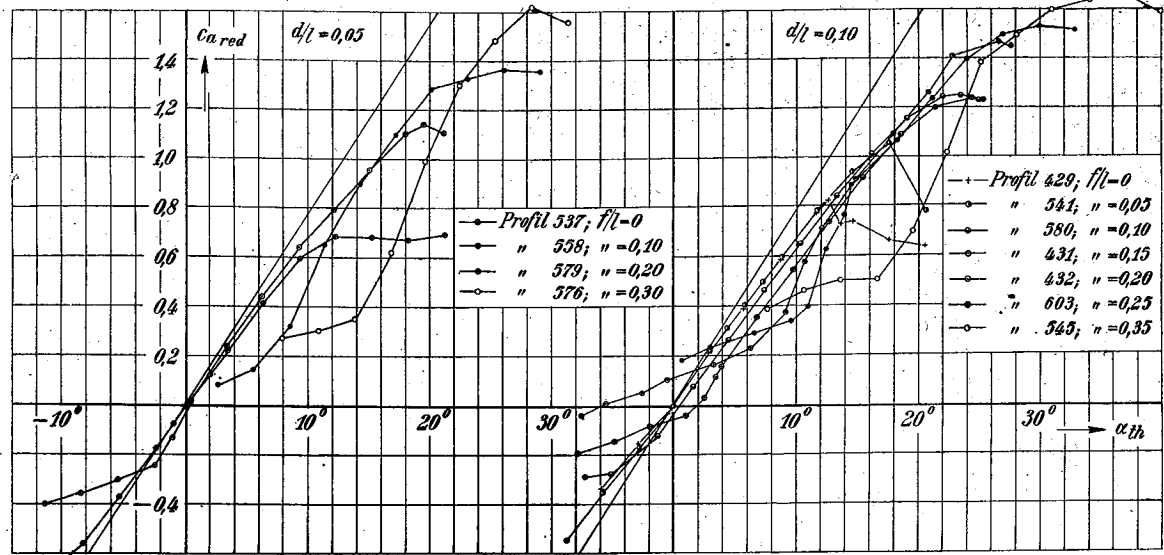


Fig. 9

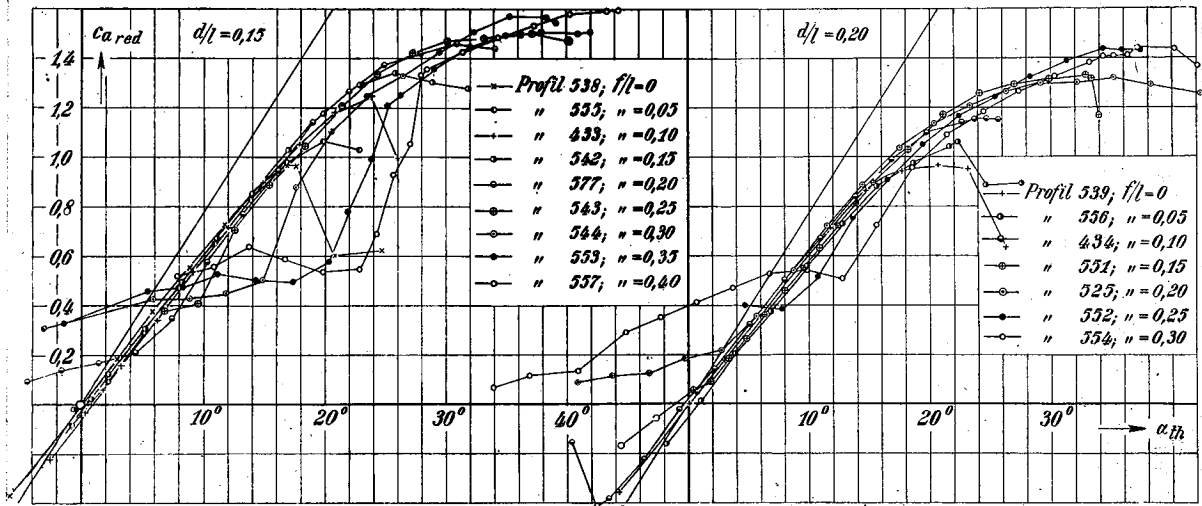


Fig. 10

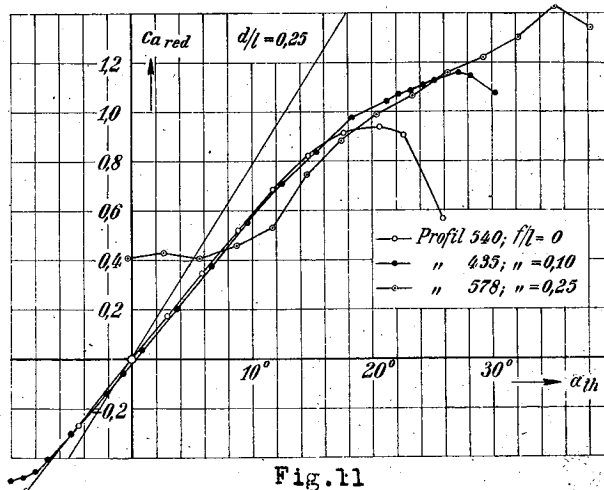


Fig. 11

Figs. 9, 10 & 11

Reduced lift coefficients in comparison with theoretical lift, as plotted against angle of attack.